Lasers in Manufacturing Conference 2019

Investigations on material removal mechanisms of steel by means of laser processing for balancing processes

Peter Hellwig[a*], Klaus Schricker[a], Jean Pierre Bergmann[a]

[a]*Technische Universität Ilmenau, Production Technology Group, Gustav-Kirchhoff-Platz 2, 98693 Ilmenau, Germany*

Abstract

Rotating parts as for example rotors for industrial application present small but undesirable unbalances after chipping. Rotors which are exposed to high rotational speeds require unbalances approaching zero. Mass corrections such as material removal has to be carried out in a short time, in order to hold a profitable cycle time. Ablation by means of laser beam allows a high quality removal, but a low removal rate. Laser-based material removal through a welding process represents a novel approach for the use in balancing processes. In this case sputter formation is purposely used, in order to enhance the material removal. In this contribution, a 1.5 kW fibre laser (cw-mode) was used for processing X5CrNi18-10 steel sheets. Spatter formation out of the molten pool was identified as primary removal mechanism. Further investigations regarding process velocity up to 10 m/s, various incidence angles of the laser beam and the number of passes were carried out. Thereby, precise weighings confirmed a sufficient removal rate for the application in balancing processes. Concluding studies were carried out regarding surface parameters, e.g. profile depth, to refer them to industrial requirements and conventional chipping methods.

Keywords: removal rate; cw-based remote welding; laser beam incidence angle; material removal of steel

1. Introduction

For balancing processes of high-speed turning rotors, it is necessary to achieve high precise mass corrections. The application of laser radiation instead of conventional chipping methods represents a novel approach in this context, when processing time can be shortened towards laser ablation.

**Corresponding author. Tel.: +49-3677-69-3866; fax: +49-3677-69-1660 .*
E-mail address: info.fertigungstechnik@tu-ilmenau.de .

The laser beam as a contactless tool offers many advantages like high flexibility as well as a totally wear- and tear free material removals. In most industrial applications, laser-based material removal is achieved by different mechanisms regarding pulsed or continues processes. In case of pulsed processes, the use of short and ultrashort pulsed laser radiation is well known, as shown for ns-pulses (Yao et al., 2005) and fs/ps-pules (Jaeggi et al., 2017).

The material removal mechanism depends strongly on the pulse length and is dominated by evaporation, melt ejection and ablation (Hügel et al., 2009). However, the use of cw-mode in material removal leads to higher removal rates compared to pulsed processes. Fusion cutting is the most widespread application of cw-mode material removal, where an assisting oxygen jet is used to blow out the melt (Yao et al., 2005). Because of permanent acceleration and deceleration phases of the linear axes for elaborate geometries, only cutting speeds of less than 20 m/min can be achieved for conventional fusion cutting (Wetzig et al., 2015). Steady developments in laser technology improves solid-state lasers, in particular their beam quality. Due to these higher beam qualities, long distance focusing objectives and beam manipulation systems it has become possible to reach processing speeds of up to 18,000 m/min (Exner et al., 2012). Another decisive advantage is that at these cutting speeds no assisting oxygen jet is necessary anymore (Siebert et al., 2014). The ablation depth mainly depends on the material properties, the focal diameter respectively intensity and the traversing velocity of the laser beam. Thereby, remote ablation cutting involves a mixture of evaporation and ejection of molten material as removal mechanisms. About 20-40% of the removed material gets evaporated which leads to a recoil pressure of the metal vapor to the molten material. This results in the acceleration of the liquid phase out of the processing zone (Zaeh et al., 2010; Musiol et al., 2012). Therefore, melt ejection (and sputter formation) can be used in order to enhance material removal in the liquid phase.

Deep penetration laser welding at high speeds and the mechanisms of spatter formation can derive a deeper examination of the interaction between melt ejection and vaporization. It is noted that for deep penetration laser welding with welding speeds above 5 m/min, the keyhole starts to incline which has a decisive impact on spatter formation. With the inclination of the keyhole, the emitted vapor jet hits the rear wall of the capillary which leads to an up warded flow of the melt. In combination with the melt flow around the keyhole this effect results in a droplet escape (Rominger, 2010; Weberpals, 2010). In further studies, it can be seen that spattering or the loss of mass also increases with steeper beam incident angles in trailing direction (Oefele, 2012). This effect is mainly based on the resulting inclination of the keyhole. Significant alterations of the weld pool geometry were observed in (Kumar et al., 2017) by applying small incident beam angles around 7°. In turn, alterations of the weld pool geometry might lead to modifications of the melt pool dynamics and thus have an influence on the spatter conditions. These effects have widely been investigated for welding speeds of up to 20 m/min (Weberpals et al., 2008; Nagel et al., 2016; Schmidt et al., 2019). It is to be investigated whether these conditions can be transferred to processes with significantly higher welding speeds.

In this paper, investigations regarding the material removing for balancing processes using cw-mode laser radiation are carried out for welding speeds up to 600 m/min. Based on the maximum material ablation rate, experiments on the effect of small incident angles and a comparison to phenomena known in laser beam welding were performed. A description of the removal mechanism is given by high speed recordings based on the number of passes. Eventually, first characterizations of the processed areas in terms of uniformity and roughness complete the investigations.

2. Experimental Setup

The experiments were carried out with stainless austenitic steel sheets 1.4301 (X5CrNi18-10; AISI 304). The dimensions of the sheets as well as the position of the processed lines and areas can be found in Fig. 1b). In order to realize the relative motion between the laser beam and the work piece of up to 600 m/min, a 1.5 kW fiber laser (FL 015, Rofin) in combination with a galvanometric scanner (intelliSCAN 20, Scanlab) was used. The beam was focused using a 163 mm focal distance F-theta lens. The technical data of the laser and scanning system are summarized in Table 1. The laser power was set to 620 W for all experiments, so that a laser beam intensity of approximately $1.5 \cdot 10^8$ W/cm² resulted.

Table 1: Technical data of the laser and scanning system

Technical data of laser and scanning system	Values
wavelength [nm]	1070
pulse repetition frequency	cw
focal diameter [µm]	23
max. laser power on work piece [W]	1500
max. scan speed [m/min]	720

The influence of longitudinal beam incidence angles is investigated by placing the samples in three different areas within the scanning field. The maximum trailing and leading incidence beam angle of the scanning system (± 3.9°) was applied by processing near the edge area of the scanning field. Fig. 1a schematically shows the application of the three different incidence beam angles with the corresponding values. The sample dimensions are shown in Fig. 1b. Investigations on single lines were used to describe the removal mechanism. The number of lines was increased accordingly for the investigations on areal material removal. The number of scans is indicated by the symbol i.

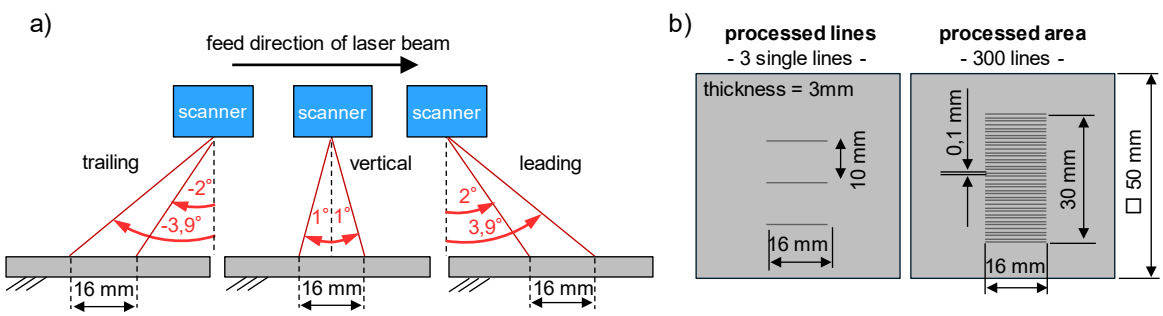

Fig. 1. (a) Different setups for the three applied beam incidence angles; (b) Sample geometry showing the processed lines (left) and processed area (right)

The weighing of the specimen in order to register the material removal from the melting pool was carried out using a precision balance with a resolution of 0.01 mg (Sartorius). The samples were weighed before and after the process to determine the loss of mass. Because of the high resolution of 0.01 mg it was necessary to clean the samples in an ultrasonic bath with acetone and isopropyl alcohol in two steps before each weighing. To observe the ejections of molten material respectively to understand the removal mechanism, high-speed recordings of the process were carried out. A high-speed camera Photron Fastcam SA-X2 (frame

rate: 50,000 frames per second, 32 gigabyte internal memory, 1.8 seconds maximum recording duration) with Polytec Navitar 12X ZoomLens objective was used. A narrow band filter for the wavelength of 808 nm was inserted into the optical path of the camera. The illumination was realized by the Cavilux HF system. A schematic view of the setup is included with the corresponding high-speed images (see Fig. 2d). For surface characterization and determination of profile depths a laser scanning microscop Olympus LEXT was used.

3. Results and discussion

3.1 Scanning speeds and ablation rates

In order to figure out at which scanning speeds the loss of mass reaches its maximum, five different speeds were applied for the experiments (60, 150, 300, 450 and 600 m/min). The investigations were carried out using the vertical beam incidence angle setup (see Fig. 1a) to process areas consisting of 300 lines with a spacing of 100 µm. Each line was passed with 4 scans to raise the loss of mass. This approach clarifies the difference in mass loss between the applied scanning speeds. The results can be seen in Fig. 2a). The lowest loss of mass of about 89 mg results for a scanning speed of 60 m/min. Then an increase up to 216 mg for a scanning speed of 150 m/min occurs. The corresponding high-speed records of the fourth scan, which are depicted in Fig. 2b, clarify the different spatter behaviors. While at scanning speeds of 60 m/min only humps are produced, higher scanning speeds leads to spatter formation. These spatters seem to get smaller with increasing scanning speed from 150 m/min to 300 m/min, which can be taken as an explanation for the difference in the loss of mass. For scanning speeds above 300 m/min the loss of mass is roughly similar. To determine the removal rate, the loss of mass was then offset against the needed process time (see Fig. 2b). Thereby, a scanning speed of 600 m/min results in the highest ablation rate of approx. 20 mg/s. For this reason, the remaining experiments of this study are carried out using a scanning speed of 600 m/min.

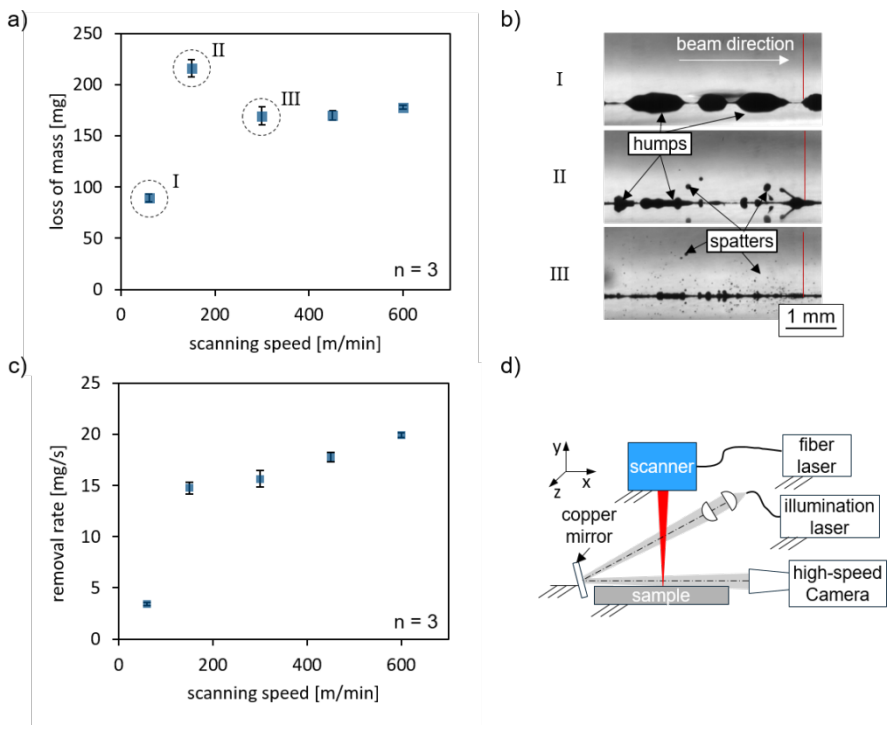

Fig. 2. (a) Effect of scanning speed on loss of mass; (b) Footage of spatter formation for different scanning speeds, (c) Influence of scanning speed on resulting removal rates, (d) Camera and illumination setup.

3.2 Different beam incidence angles

Samples were processed using the previously determined scanning speed of 600 m/min to determine the effect of different beam incidence angles on the ablation rate. For these trials, the areal setup (see Fig. 1b)) was applied while passing every line by four scans. The resulting ablation rate for the different incidence angles are depicted in Fig. 3. It becomes apparent that the loss of mass is 5.9 % higher with applying the trailing incidence angle. The leading incidence angle results in a 3.1 % lower ablation rate compared to the vertical beam incidence. The increase in loss of mass with trailing beam angles could be explained by the inclination of the keyhole (Weberpals, 2010; Oefele, 2012). With an inclined capillary the recoil pressure of the evaporated material from the front wall hits the circulating melt flow of the rear keyhole wall at high velocity. This leads to a formation of melt pool swellings. Through friction effects between the outflowing metal vapor and this melt pool swellings, ejections of the molten material are created. For leading beam incidence angles the keyhole is inclined in beam direction. Thus, the metal vapor flow is directed to the bottom of the keyhole where it is decelerated by the rear wall and leads to less melt pool swellings compared to the trailing incidence angle. The results seem to make these state-of-the-art observations applicable for the investigated high welding speeds as well, but further investigations will follow.

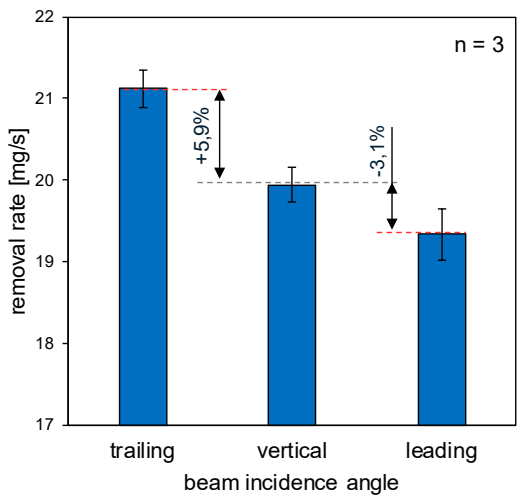

Fig. 3. Influence of beam incidence angles on resulting removal rates. Processed areas, scanning speed = 600 m/min, number of scans i = 4

It is to be assumed that the characteristics of the values are that low because of the relatively small applied incident angles. Differences in kerf depth are depicted in Fig. 4. In Oefele, 2012 for example, it was calculated and experimentally confirmed that deviations of beam incidence angles from -45° up to 20° leads to negligible changes in weld seam depth. Fig. 4a compares the cross sections of the resulted kerfs after the first and fourth scan. It can be seen that a small layer of molten material with thicknesses around 10 µm stays on the bottom of every kerf. In addition, re-deposition and re-solidification of molten material can be observed at the kerf walls which leads to decreased ablation rates. The values for the measured kerf depths are shown in Fig. 4b. It can be seen that the resulting kerf depth for the trailing angle, especially after four scans is slightly higher than for the vertical and leading beam application. After the first scan there is no significant difference in kerf depth visible, regarding the beam incidence angle. However, there is a significant difference in kerf depth after the first and fourth scan.

If, for example, only the trailing angle is considered, a 33 µm deep kerf results after the first scan and an approximately four times higher depth (128 µm) after the fourth one. This leads to the assumption, that there is an almost linear correlation between the number of scans and the kerf depth for the applied four passes. Whether this functional relationship also applies to higher numbers of scans, must be proofed with further examinations. It can be assumed that the displacement of the surface to be machined will cause lower laser beam intensities, which are then no longer sufficient for melting the material.

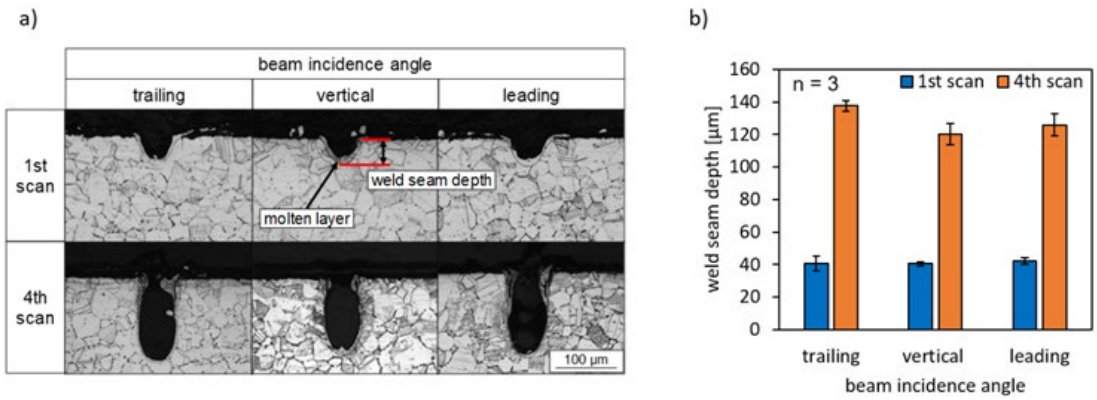

Fig. 4. (a) Cross sections of ablated kerfs for the trailing, vertical and leading incidence angle after the first and fourth scan. (b) Influence of beam incidence angles on kerf depth.

To investigate the loss of mass and the stepwise formation of the kerfs, the melt ejections were characterized by high-speed recordings for every pass. For the visualization of the ejections from the melt pool it was necessary to illuminate the process from the rear directly into the optical path of the camera objective. That is the reason because the ejections shown in Fig. 5 and Fig. 2b are merely the shadows of those. The footage of the spatter behavior (see Fig. 5) indicates, that the size and angle of spatter detachment changes with increasing number of scans.

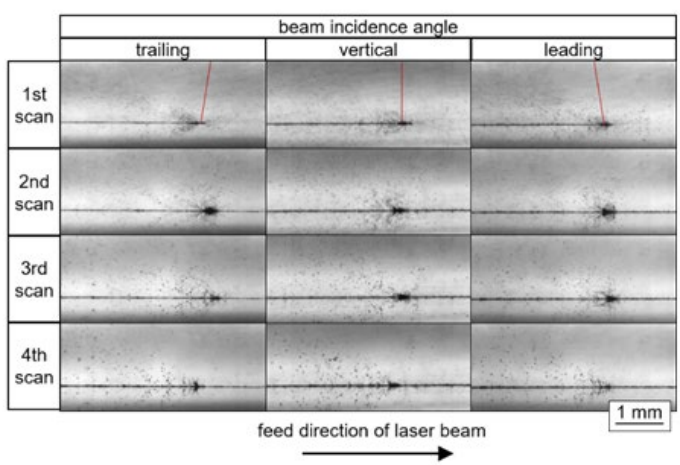

Fig. 5. Footage of high-speed recordings for the different beam incidence angles during the first, second, third and fourth scan. scanning speed = 600 m/min

At the first two scans of the laser beam, relatively small spatters can be detected. With increasing number of scans, the size of the spatters increases as it is to be seen for the third and fourth scan. What all the pictures have in common is the direction of the spatter formation, which is against the feed direction of the laser beam. The angle of spatter detachment seems to get smaller with increasing number of scans. However, the application of the deviated incidence angles has no visible influence on the characteristics of melt ejections.

3.3 Surface evaluation

The following part shows the first observations of the resulting surface characteristics. For this purpose, the laser-scanning-microscope was used as well as cross section. Fig. 6a shows a cross section, surface profiles of three measuring planes at different y-positions (Fig. 6b) and a three-dimensional laser-scanning-microscopy of an areal processed sample (Fig. 6c). It should be noted that the cross section is only a snapshot and does not correspond with the measuring planes for the profiles directly. The melt solidifications at the kerf walls prevent a complete and reliable recording of the entire kerf geometries for the laser scanning microscope. Nevertheless, it can be seen that the depths of the profiles are in the range of about 160 µm.

For the implementation of the examined material removal process in balancing applications certain surface qualities have to be reached. For that reason, further experiments are planned to develop strategies to improve the surface quality. These investigations will include the influence of various line spacing and certain overlaps as well as stepwise rotational overlaps on the resulting surface, e.g. R_a or R_z as roughness parameters.

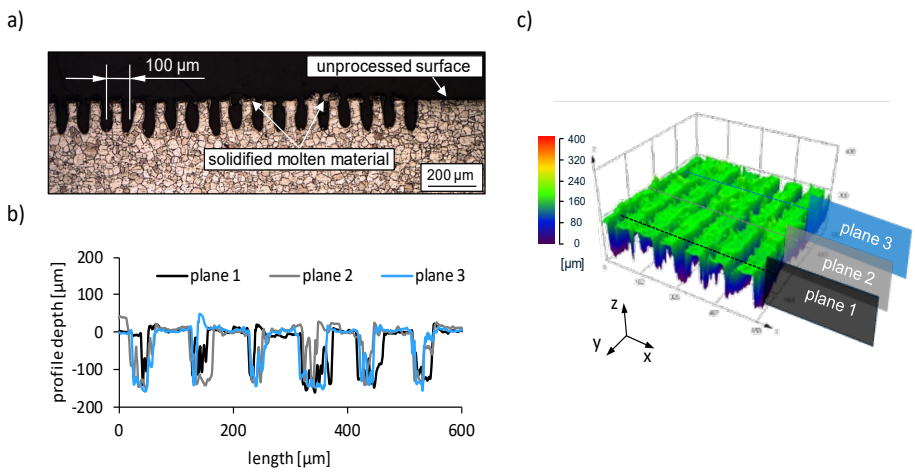

Fig. 6. (a) Cross section of a processed area; (b) kerf profiles of three measured planes; (c) 3d-laser scanning microscopy of processed area; number of scans i = 4; scanning speed = 600 m/min; spacing = 100 µm; beam incidence angle = vertical.

4. Conclusions

In this paper, the material removal mechanism of steel by means of cw-mode laser radiation was examined experimentally by detecting the loss of mass, observation of melt ejections with high-speed recordings and cross sections. The application of the highest examined scanning speed of 600 m/min resulted in the highest ablation rate of approximately 20 mg/s. Furthermore, the influence of small longitudinal leading and trailing beam incidence angles from 2.0° to 3.9° on the ablation rate and resulting kerf depths was investigated. At small trailing incidence angles there was a low increase of 5.9 % in ablation rate. Therefore, it can be assumed that an inclination of the keyhole leads to altered beam reflection and absorption conditions. The developed camera and illumination setup enabled a lateral view on the process. Thus, it was possible to observe an increase in the size of the melt ejections with increasing number of scans. First characterizations of the areal processed samples were made which shows reproducible kerf depths.

Future investigations will focus on observations of the keyhole aperture and the dimensions of the weld pool by the application of coaxial high-speed recordings. Furthermore, methods will be developed for a more comprehensive characterization of the melt ejections by image processing. Beyond that, further investigations will give a detailed look on strategies to improve the surface quality.

Acknowledgements

The authors gratefully acknowledge support and funding from the European Regional Development Fund (EFRE) grant no. 2017 FE 9091. We would also like to thank Prof. Dr.-Ing. Jens Bliedtner for the opportunity to carry out parts of the experiments at Ernst-Abbe-Hochschule Jena.

References

Exner, H., Hartwig, L., Ebert, R., Kloetzer, S., Streek, A., Schille, J., Loeschner, U., 2012. High Speed Laser Micro Processing Using High Brilliance Continuous Wave Laser Radiation, Journal of Laser Micro/Nanoengineering, Vol. 7.

Hügel, H., Graf, T., 2009. Laser in der Fertigung – Strahlquellen, Systeme, Fertigungsverfahren.

Jaeggi, B., Neuenschwander, B., Remund, S., Kramer, T., 2017. „Influence of the pulse duration and the experimental approach onto the specific removal rate for ultra-short pulses“, Laser Applications in Microelectronic and Optoelectronic Manufacturing, Proc. of SPIE Vol. 10091.

Kumar, N., Mukherjee, M., Bandyopadhyay, A., 2017. Study on laser welding of austenitic stainless steel by varying incident angle of pulsed laser beam. Optics and Laser Technology 94, p. 29-309.

Musiol, J., Luetke, J., Schweier, M., Hatwig, J., Wetzig, A. et al., 2012. Combining remote ablation cutting and remote welding: opportunities and application areas. High Power Laser Materials Processing, Proc. of SPIE Vol. 8239.

Nagel, F., Stambke, M., Bergmann, J.P., 2016. „Reduction of spatter formation by superposition of two laser intensities”. ICALEO 2016.

Oefele, F., 2012. Remote-Laserstrahlschweißen mit brillianten Laserstrahlquellen, Technische Universität München, PhD thesis.

Rominger, V., Schäfer, P., Weber, R., Graf, T., 2010. Prozessuntersuchungen beim Laserstrahltiefschweißen – Festkörperlaser hoher Brillanz im Vergleich zu CO_2-Lasern, DVS-Berichte, Band 267, p. 188-193.

Schmidt, L., Hickethier, S., Schricker, K., Bergmann, J.P., 2019. „Low-spatter high speed welding by use of local shielding gas flows”, High-Power Laser Materials Processing: Apllications, Diagnostics, and Systems. Proc. of SPIE Vol. 10911

Siebert, R., Baumann, R., Beyer, E., Herwig, P., Wetzig, A., 2014. „Laser Manufacturing of Electrical Machines“, 4th International Electric Drives Production Conference (EDPC)

Weberpals, J.-P., Dausinger, F., 2008. Fundamental understanding of spatter behavior at laser welding of steel. ICALEO 2008, p.364-373.

Weberpals, J.-P., 2010. Nutzen und Grenzen guter Fokussierbarkeit beim Laserschweißen, Universität Stuttgart, PhD thesis.

Wetzig, A., Baumann, R., Herwig, P., Siebert, R., Beyer, E., 2015. „Laser remote cutting of metallic materials: opportunities and limitations“, Industrial Laser Applications Symposium, Proc. of SPIE Vol. 9657.

Yao, Y.L., Chen, H., Zhang, W., 2005. Time scale effects in laser material removal: a review, International Journal of Advanced Manufacturing Technology 26, p. 598-608.

Zaeh, M. F., Musiol, J., Moesl, J., 2010. “Methodical qualification of scanner systems for remote laser cutting”, International Congress on Applications of Lasers & Electro-Optics. ICALEO 2010, no. 362.